ACS Chemical Neuroscience

pubs.acs.org/chemneuro Research Article

Ligand-Induced Stabilization of the Native Human Superoxide Dismutase 1

Karoline Santur, Elke Reinartz, Yi Lien, Markus Tusche, Tim Altendorf, Marc Sevenich, Gültekin Tamgüney, Jeannine Mohrlüder,* and Dieter Willbold*

Cite This: https://doi.org/10.1021/acschemneuro.1c00253 Read Online

ACCESS | Metrics & More | Article Recommendations

ABSTRACT: A common characteristic of familial (fALS) and sporadic amyotrophic lateral sclerosis (sALS) is the accumulation of aberrant proteinaceous species in the motor neurons and spinal cord of ALS patients—including aggregates of the human superoxide dismutase 1 (hSOD1). hSOD1 is an enzyme that occurs as a stable dimeric protein with several post-translational modifications such as the formation of an intramolecular disulfide bond and the acquisition of metal cofactors that are essential for enzyme activity and further contribute to protein stability. Some mutations and/or destabilizing factors promote hSOD1 misfolding, causing neuronal death. Aggregates containing misfolded wild-type hSOD1 have been found in the spinal cords of sALS as well as in non-hSOD1 fALS patients, leading to the hypothesis that hSOD1 misfolding is a common part of the ALS pathomechanism. Therefore, stabilizing the native conformation of SOD1 may be a promising approach to prevent the formation of toxic hSOD1 species and thus ALS pathogenesis. Here, we present the 16-mer peptide S1VL-21 that interferes with hSOD1 aggregation. S1VL-21 was identified by phage display selection with the native conformation of hSOD1 as a target. Several methods such as microscale thermophoresis (MST) measurements, aggregation assays, and cell viability assays revealed that S1VL-21 has a micromolar binding affinity to native hSOD1 and considerably reduces the formation of hSOD1 aggregates. This present work therefore provides the first important data on a potential lead compound for hSOD1-related drug development for ALS therapy.

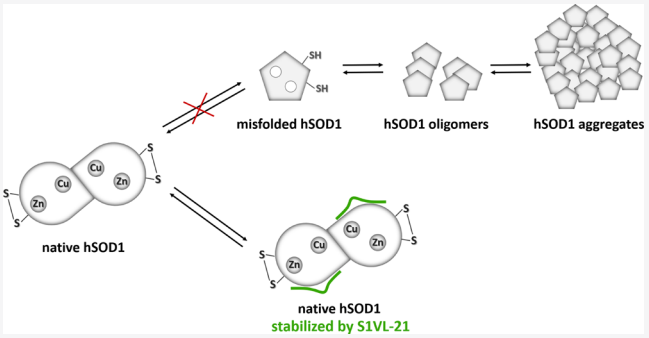

KEYWORDS: *ALS, SOD1, aggregate elimination, treatment strategy, native conformation stabilization, phage display selection*

INTRODUCTION

Amyotrophic lateral sclerosis (ALS) is a fatal adult-onset neurodegenerative disorder that causes degeneration of upper and lower motor neurons in the primary cortex, brain stem, and spinal cord. Death occurs typically within 3−5 years after diagnosis due to respiratory failure. Approximately 90% of all ALS cases are considered sporadic (sALS), whereas familial ALS cases (fALS) account for the remaining ∼10%.[1−3] However, despite widespread research, there is still no efficient treatment for ALS. The only available FDA approved drugs are riluzole and radicava, which extend survival by only 2−3 months[4] or decelerate the rate of decline in physical functions by 33%,[5] respectively.

Mutations in the gene coding for the human superoxide dismutase 1 (hSOD1) are found in ∼1% of all ALS cases[6] and account for ∼20% of fALS cases.[5] Since 1993, when the first ALS-associated mutations in hSOD1 were found,[7] more than 200 mutations in hSOD1 have been identified (https://alsod.ac.uk/). The human SOD1 is an enzyme that converts toxic superoxide radicals to hydrogen peroxide and oxygen. The mature protein is a 32 kDa homodimer with one copper and one zinc ion per monomer that are important for the activity and stability, respectively. An intramolecular disulfide bond in each subunit further contributes to protein stability.[8] All post-translational modifications, including the dimerization, the coordination of the metals, and the disulfide bond, lead to one of the most stable proteins known.[9,10] However, mutations and/or altered post-translational modifications are linked to the pathogenesis of ALS, whereas the underlying mechanism behind hSOD1-mediated toxicity is still unclear. Loss of hSOD1 function may lead to an accumulation of toxic radicals and thus be a possible reason for the disease, but SOD1 knockout mice do not exhibit an ALS-like phenotype.[11] Some studies have suggested a toxic gain-of-function of mutant hSOD1 as a result of protein misfolding and aggregation,[8,12,13]

Received: April 20, 2021
Accepted: June 1, 2021

and the pathogenicity of mutant hSOD1 is proportional to the amount of toxic hSOD1 species.[14] Indeed, aggregates containing mutant and misfolded hSOD1 have been found in the spinal cord of sALS and hSOD1-fALS patients.[15−17] In addition, misfolded wild-type hSOD1 was also detected in non-hSOD1 fALS patients leading to the hypothesis that hSOD1 misfolding is a common part of the ALS pathomechanism.[18] Moreover, aggregated hSOD1 has been shown to induce aggregation of mutant and wild-type SOD1 *in vitro*[19] as well as in cell culture[20] with a prion-like behavior[21] and the overexpression of wild-type hSOD1 in mice led to an ALS-like phenotype.[13] Lacking one or several post-translational hSOD1 modifications destabilizes the native protein and generates an apo monomer, whose thermal stability is significantly reduced, and that has been shown to be the precursor for aggregation.[22,23]

In order to investigate whether the destabilization of the hSOD1 holoenzyme is crucial to ALS pathology, we want to explore whether stabilization of the native hSOD1 conformation by specifically binding ligands is able to interfere with hSOD1 aggregation. Such ligands should then be able to inhibit formation of hSOD1 aggregates *in vitro* and *in vivo*. In addition, elimination of pre-existing hSOD1 aggregates might also become feasible.

A similar approach has been applied in the transthyretin (TTR)-associated amyloidosis. It has been shown that the tetrameric protein dissociates into monomers before misfolding and aggregation.[24] However, binding of small specific molecules stabilized the native conformation of the protein and increased the kinetic barrier to tetrameric dissociation, thus preventing amyloidosis.[25] The efficacy of specific ligands in interfering with protein aggregation was also successfully demonstrated for amyloid-β protein (Aβ), whose toxic species are involved in the pathogenesis of Alzheimer's disease. *In vitro* data revealed that the D-enantiomeric peptide RD2 binds monomeric Aβ(1−42) and inhibits concentration-dependent formation of Aβ fibrils. In addition, RD2 was able to eliminate pre-existing toxic Aβ oligomers,[26] and mouse studies demonstrated a significant reduction of Aβ oligomers as well as an improvement of cognitive properties.[26−28] Thus, stabilizing the wild-type hSOD1 native conformation by specifically binding ligands may be a beneficial approach in ALS treatment.

Here, we report the identification of a hSOD1-binding peptide selected by phage display and its analysis regarding its potential to stabilize native hSOD1 and thus inhibit hSOD1 aggregation.

RESULTS AND DISCUSSION

hSOD1-Binding Peptides Were Enriched during Phage Display Selection. To identify peptide ligands that are able to stabilize the native conformation of hSOD1, the TriCo-16 phage display peptide library was used in a phage display selection. After four selection rounds, the success of the selection was analyzed by an enrichment ELISA.

As shown by ELISA analysis (Figure 1), the phage display selection enriched phages that bind to hSOD1-coated wells (Figure 1; dark green) more than to noncoated wells (Figure 1; light green). The weak binding of the wild-type phage to hSOD1 with an intensity similar to the control without phages indicates that the measured values result from the binding of the presented peptides and not from that of the phage itself. The signal intensity of the wells with and without hSOD1 are not considerably different. As shown by the increased signal intensity with each selection round starting from the library, hSOD1-binding peptides accumulated during the selection. The library already contains hSOD1-binding peptides as indicated by the higher signal intensity for hSOD1-coated wells compared to noncoated wells.

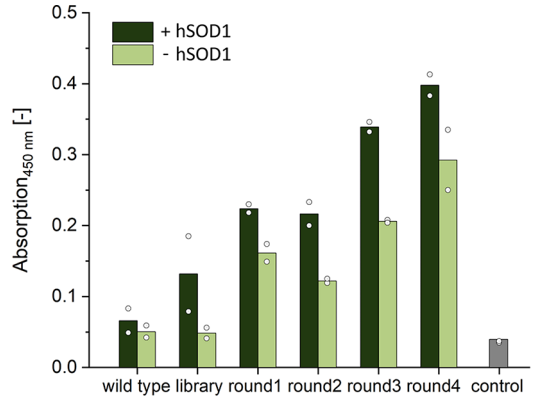

Figure 1. hSOD1-binding peptides were enriched during phage display selection. Enrichment ELISA of the hSOD1 phage display was performed to verify the enrichment of hSOD1-binding peptides during the selection. Relative binding affinities of the phage samples ($5 * 10^{10}$ phages) of the wild type, library, and each selection round to immobilized hSOD1 (dark green) and to empty wells without hSOD1 (light green) were investigated in a double determination (points: corresponding values) as well as a control without hSOD1 and phages (gray).

Sequence Analysis Led to the Identification of hSOD1-Binding Peptide S1VL-21. Next-generation sequencing (NGS) analysis followed by processing via the Target Sequencing Analysis Tool (TSAT) and Hammock led to the identification of the peptide S1VL-21. In total, 60 937 sequences were identified during this selection after analysis. The sequence at position 1 in the scoring according to the parameter Empty Score (EmS) exhibited a value of 83 but displayed an Enrichment Factor (EnF) value of only 6. In contrast, another sequence with an EnF value of 271 was most enriched, whereby this sequence was also highly present in the controls (EmS of 6). S1VL-21 was ranked at position 25 in the scoring according to the parameter EmS (value of 23) and at position 38 according to the parameter EnF (value of 25). Moreover, it formed the largest cluster in sequence alignment with 2469 sequences including 2393 unique sequences of the remaining 60 751 sequences. Thus, the peptide S1VL-21 and its three randomized control peptides S1VL-21_Rdm1, S1VL-21_Rdm2, and S1VL-21_Rdm3 were further investigated according to their potential to bind and stabilize native hSOD1 as well as their potential to prevent hSOD1 from aggregation.

S1VL-21 Exhibits Micromolar Binding Affinity to hSOD1. Microscale thermophoresis (MST) measurements were used to determine the equilibration dissociation constant (K_D) of hSOD1 to the selected peptide S1VL-21. As a control for the sequence specificity of the binding affinity, three peptides with the same amino acid residues, but in randomized sequence order, where also measured for affinity to hSOD1 (Figure 2A). Therefore, 250 nM hSOD1 labeled with CF633 was used, whereas nonlabeled peptide was added with different concentrations. The S1VL-21 exhibits the strongest binding affinity to hSOD1 with a resulting K_D of 5.3 ± 0.3 μM (Figure

https://doi.org/10.1021/acschemneuro.1c00253
ACS Chem. Neurosci. XXXX, XXX, XXX−XXX

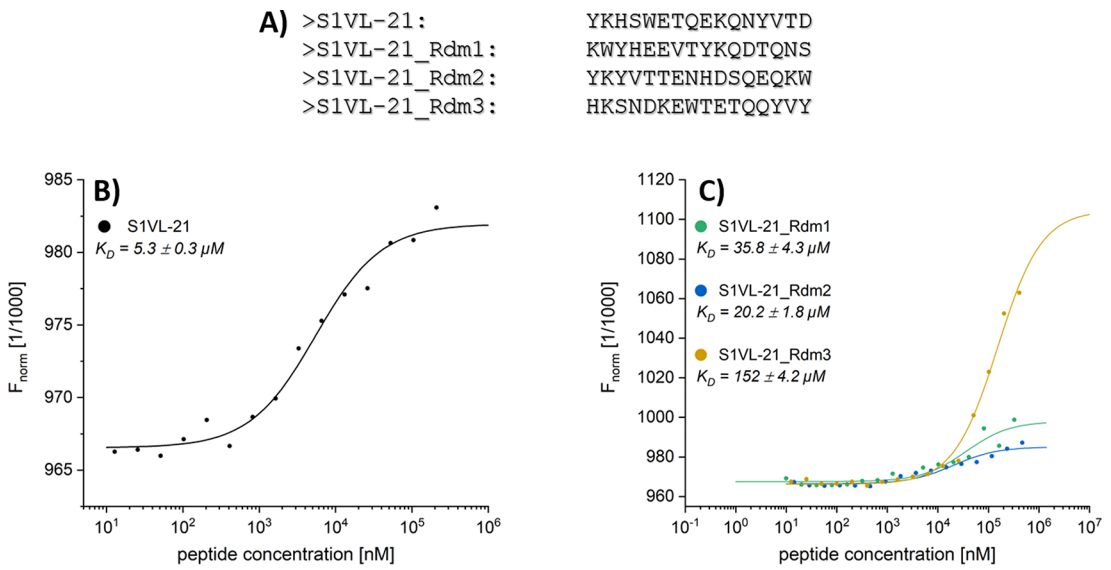

Figure 2. S1VL-21 exhibits a micromolar binding affinity to hSOD1. (A) Sequences of the selected peptide S1VL-21 and its randomized control peptides S1VL-21_Rdm1, S1VL-21_Rdm2, and S1VL-21_Rdm3, which were measured for affinity to hSOD1. (B) MST measurement of hSOD1-CF633 (250 nM) and S1VL-21 as well as (C) its randomized control peptides with increasing concentrations (10 nM−470 μM) in 50 mM sodium acetate buffer pH 6 containing 150 mM NaCl and 0.05% Tween-20 were performed at 25 °C with an LED power of 40%. Changes in thermophoresis at 40% MST power were plotted against the peptide concentrations and evaluated through thermophoresis for determining the K_D values of 5.3 ± 0.3 μM for S1VL-21 (B) and 35.8 ± 4.3 μM (C; green), 20.2 ± 1.8 μM (C; blue), and 152 ± 4.2 μM (C; orange) for the randomized control peptides S1VL-21_Rdm1, S1VL-21_Rdm2, and S1VL-21_Rdm3, respectively.

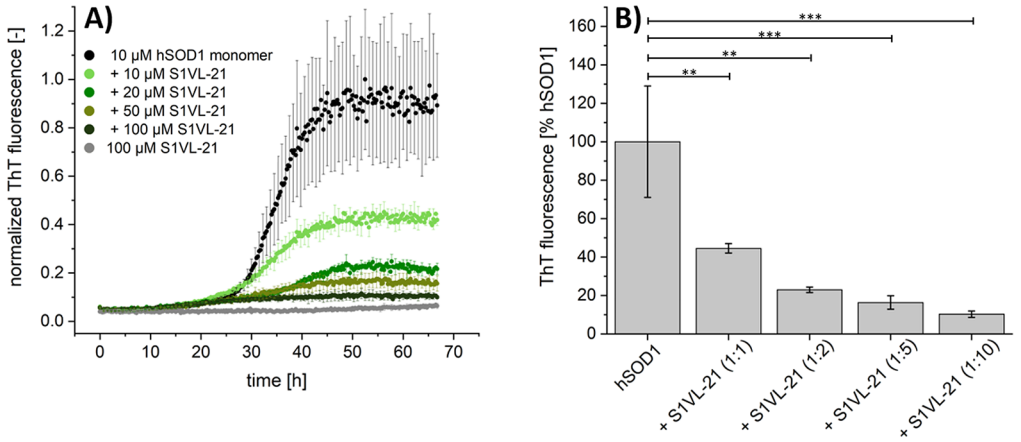

Figure 3. S1VL-21 exhibits an influence on the formation of amyloid-like hSOD1 aggregates. The ThT assay was performed to investigate the influence of S1VL-21 on amyloid-like hSOD1 aggregation. All samples containing 5 μM dimeric hSOD1 with and without the corresponding peptide concentration as well as peptide alone were incubated in 50 mM sodium acetate buffer pH 6 with 10 mM TCEP, 5 mM EDTA, 150 mM sodium chloride, and 5 μM ThT for 15 min at 37 °C before the fluorescence progression measurement was started in a 96-well half-area flat-bottom microplate (Corning, New York, USA) containing one stainless steel bead (3.2 mm). The progression of fluorescence intensity was measured every 15 min at λ_{ex} = 448 nm and λ_{em} = 482 nm with 30 s of agitation at 400 rpm before every measurement using a microplate reader (BMG Labtech, Ortenberg, Germany). The ThT fluorescence intensity was normalized to the highest value and plotted against the time. (A) The ThT assay of hSOD1 (black) and with different concentrations of S1VL-21 (green colors) in 3- to 5-fold determination. Gray: 100 μM S1VL-21 without hSOD1. The ThT fluorescence is decreased with S1VL-21. (B) Comparison of the ThT fluorescence intensity (Figure 3A) of all samples present in A after 52.5 h. S1VL-21-containing samples were normalized to the fluorescence intensity of the sample with hSOD1 alone. One-way ANOVA (analysis of variance) with Fisher post hoc analysis was used for statistical analysis. ** $p \leq 0.01$; *** $p \leq 0.001$. The ThT fluorescence was significantly reduced by 90% by addition of a 10-fold molar excess of S1VL-21.

2B). In contrast, the measurements with the randomized control peptides S1VL-21_Rdm1, S1VL-21_Rdm2, and S1VL-21_Rdm3 led to K_D values of 36, 20, and 152 μM, respectively (Figure 2C). Thus, the selected S1VL-21 has an enhanced affinity with a 4- to 30-fold lower K_D value for the hSOD1 interaction compared to the randomized control peptides.

S1VL-21 Exhibits an Influence on the Formation of Amyloid-Like hSOD1 Aggregates. To investigate the influence of S1VL-21 on amyloid-like hSOD1 aggregation, a thioflavin T (ThT) assay was performed. Briefly, 5 μM dimeric hSOD1 was incubated with and without the corresponding peptide in 50 mM sodium acetate buffer pH 6 containing 10 mM TCEP, 5 mM EDTA, 150 mM sodium chloride, and 5 μM ThT for 15 min at 37 °C before the fluorescence progression measurement was started in a microplate containing one 3.2 mm stainless steel bead per well. The

https://doi.org/10.1021/acschemneuro.1c00253
ACS Chem. Neurosci. XXXX, XXX, XXX−XXX

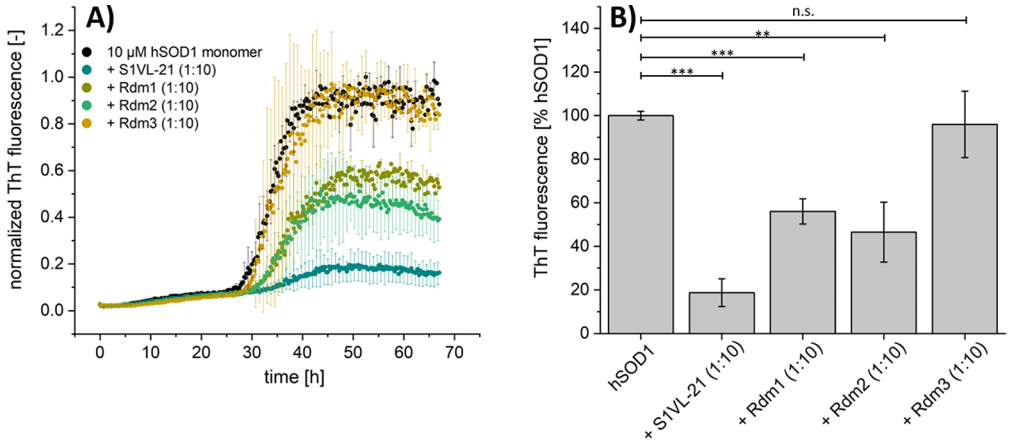

Figure 4. Randomized control peptides S1VL-21_Rdm1−3 revealed to be less effective in the inhibition of amyloid-like hSOD1 aggregation compared to S1VL-21. The ThT assay was performed to investigate the influence of S1VL-21 as well as its randomized control peptides S1VL-21_Rdm1−3 on amyloid-like hSOD1 aggregation. All samples containing 5 μM dimeric hSOD1 with and without the corresponding peptide were incubated in 50 mM sodium acetate buffer pH 6 with 10 mM TCEP, 5 mM EDTA, 150 mM sodium chloride, and 5 μM ThT for 15 min at 37 °C before the fluorescence progression measurement was started in a 96-well half-area flat-bottom microplate (Corning, New York, USA) containing one stainless steel bead (3.2 mm). The progression of fluorescence intensity was measured every 15 min at λ_{ex} = 448 nm and λ_{em} = 482 nm with 30 s of agitation at 400 rpm before every measurement using a microplate reader (BMG Labtech, Ortenberg, Germany). The ThT fluorescence intensity was normalized to the highest value and plotted against the time. (A) The ThT assay of hSOD1 (black) was performed in a 3-fold determination with a 10-fold molar excess of peptides (100 μM; other colors) related to the monomeric concentration of hSOD1. The peptides alone showed no increase in fluorescence (data not shown). The ThT fluorescence is most reduced with S1VL-21. (B) Comparison of the ThT samples after 52.5 h. Samples containing peptides are normalized to the fluorescence of the sample with hSOD1 alone. One-way ANOVA (analysis of variance) with Fisher post hoc analysis was used for statistical analysis. ** $p \leq 0.01$; *** $p \leq 0.001$; n.s. not significant ($p > 0.05$). The ThT fluorescence was significantly reduced by 44 and 53% with a 10-fold molar excess of S1VL-21_Rdm1 and S1VL-21_Rdm2, respectively. S1VL-21_Rdm3 did not reduce the ThT fluorescence.

effect of S1VL-21 on hSOD1 aggregation was determined by adding increasing concentrations of S1VL-21 to the fibrillation samples. Furthermore, the randomized control peptides were also analyzed for their influence on amyloid-like hSOD1 aggregate formation. In order to exclude aggregation of the peptide itself, the respective peptide was also investigated under the given conditions without hSOD1. Due to the high concentrations of TCEP and EDTA, which reduces the disulfide bond and complexes the metal ions, respectively, and the given stainless steel bead that causes mechanical agitation and thus fragmentation, hSOD1 unfolds and aggregates.[29]

The results were analyzed by comparing the relative fluorescence emission after 52.5 h, where the control (without peptide) reached its fluorescence maximum (Figure 3A; black). As shown in Figure 3A, the maximal fluorescence emission was decreased by addition of S1VL-21, and this effect was more evident the more peptide was added. With a 10-fold molar excess, the fluorescence was reduced by 90% (Figure 3B).

Compared to S1VL-21, its randomized peptides S1VL-21_Rdm1, S1VL-21_Rdm2, and S1VL-21_Rdm3 indicated less influence on ThT fluorescence and thus on the formation of amyloid-like hSOD1 aggregates as shown in Figure 4. While S1VL-21_Rdm1 and S1VL-21_Rdm2 reduced the plateau of the hSOD1 aggregation-dependent ThT fluorescence by about 44 and 53%, respectively, S1VL-21_Rdm3 did not exhibit any effect at all (Figure 4B). Thus, the randomized control peptides with the same amino acid composition but in a different sequence order were less effective in inhibition of amyloid-like hSOD1 aggregation compared to S1VL-21.

Incubation of hSOD1 with S1VL-21 during Aggregation Resulted in hSOD1 Species That Were Significantly Less Toxic to Neuro2a Cells than Non-peptide-Treated hSOD1 Aggregates. In order to confirm that resulting hSOD1 species are less toxic to Neuro2a cells when hSOD1 was incubated with S1VL-21 under reducing conditions during the aggregation assay, a cell viability assay using the reduction of MTT was performed in a 5-fold determination (Figure 5). Therefore, Neuro2a cells were treated with samples that have been collected after 65 h of hSOD1 aggregation incubated with and without increasing concentrations of S1VL-21.

The cell proliferation was normalized to the mean value of cells treated with medium. Subsequently, the rate of cells that were rescued due to the initial addition of S1VL-21 during hSOD1 aggregation was determined by normalizing the proliferation level to that of cells treated with hSOD1 aggregates. Cells treated with hSOD1 that has been incubated with different concentrations of S1VL-21 during the aggregation assay yielded a concentration-dependent increase in rescue rate (Figure 5; 1:1:14 ± 6%; 1:5:35 ± 7%; 1:10:48 ± 8). Notably, compared to cells treated with hSOD1 aggregates, 48% of cells have been rescued after treatment with hSOD1 species, where hSOD1 was initially incubated with a 10-fold molar excess of S1VL-21. Thus, the incubation of hSOD1 with S1VL-21 during the aggregation assay resulted in hSOD1 species that were significantly less toxic to Neuro2a cells than non-peptide-treated hSOD1 aggregates.

CONCLUSION

It has been shown that destabilizing of hSOD1 by mutations and/or post-translational modifications possibly leads to hSOD1 misfolding and aggregation, whereas *in vitro* and *in vivo* studies revealed an important role of hSOD1 aggregates in the progression of ALS. These aggregates containing mutant and misfolded wild-type hSOD1 were found in sALS patients

https://doi.org/10.1021/acschemneuro.1c00253
ACS Chem. Neurosci. XXXX, XXX, XXX−XXX

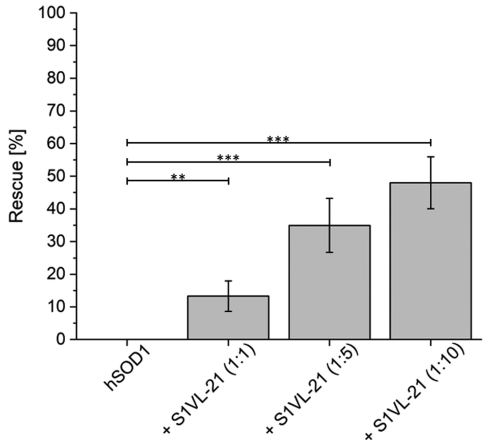

Figure 5. Incubation of hSOD1 with S1VL-21 during aggregation resulted in significantly less toxic hSOD1 species to Neuro2a cells than non-peptide-treated hSOD1 aggregates. A cell viability assay was performed in Neuro2a cells (2500 cells/well) cultured in flat-bottomed 96-well plates in DMEM including 10% FBS and 1% streptomycin and penicillin. After 6 h, the cells were treated with the pellet of samples containing hSOD1 alone and hSOD1 that was incubated with increasing concentrations of S1VL-21 during 65 h under aggregating conditions as described in Figure 3. Therefore, the samples were centrifuged at 100 000*g* for 1 h at 4 °C, and the pellet was solvated and diluted (1:1) in medium. After 3 days, the cell viability was measured using the cell proliferation Kit I according to the manufacturer's instructions (Roche, Basel, Switzerland) in a 5-fold determination. The proliferation was normalized to the mean value of the medium-treated cells. The rate of cells that could be rescued due to the initial addition of S1VL-21 during hSOD1 aggregation was determined by normalizing the proliferation level to that of cells treated with hSOD1 aggregates. One-way ANOVA (analysis of variance) with Fisher post hoc analysis was used for statistical analysis. ** $p \leq 0.01$; *** $p \leq 0.001$. Cells treated with hSOD1 that has been incubated with different concentration of S1VL-21 during aggregation led to a concentration-dependent increase in the rescue rate compared to non-peptide-treated hSOD1 aggregates.

as well as in hSOD1-fALS and non-hSOD1 fALS patients.[8,16,18]

Our intention was to explore whether stabilization of the native hSOD1 conformation by specifically binding ligands is able to interfere with hSOD1 aggregation.

Here, we report a 16-mer peptide S1VL-21 selected by phage display that was identified as a ligand to stabilize the native conformation of hSOD1. MST measurements revealed a micromolar binding affinity of S1VL-21 to native hSOD1. ThT assays were used to investigate the inhibition efficacy of S1VL-21 on hSOD1 aggregation. As the emission at 482 nm is proportional to the amount of amyloid fibrils and amyloid-like aggregates, the aggregation of hSOD1 was followed by measuring the ThT fluorescence.[30] We observed that coincubation of hSOD1 with S1VL-21 during the aggregation assay resulted in a concentration-dependent inhibition of the ThT fluorescence emission increase. For example, incubation of hSOD1 with an equimolar amount of S1VL-21 under hSOD1-aggregating conditions resulted in a reduced formation of amyloid-like hSOD1 aggregates by 55%, whereas with a 10-fold molar excess of S1VL-21, the formation of amyloid-like hSOD1 aggregates was reduced by even 90%. Additionally, we were able to show that these remaining species are less toxic to Neuro2 cells than non-peptide-treated hSOD1 aggregates, also in a concentration-dependent manner, probably due to the lower amount of aggregates. Although the mechanism of hSOD1 aggregation has not yet been clearly elucidated, Chattopadhyay et al. demonstrated *in vitro* that even small amounts of metal-free and reduced monomeric hSOD1 can initiate the formation of amyloid species in disulfide-bridge-intact forms of hSOD1 and that elongation is driven by recruitment of apo or partially metalated, dimeric, disulfide-intact hSOD1.[31] We suggest that the specific binding of S1VL-21 to the native hSOD1 leads to a reduction or even a prevention in the formation of misfolded, ThT-positive hSOD1 species. Moreover, the effect of S1VL-21 is sequence-specific as indicated by the analyses using sequence randomized control peptides. Whereas Rdm1 and Rdm2 also showed a reducing but considerably smaller effect on the formation of amyloid-like hSOD1 aggregates compared to S1VL-21, Rdm3 did not exhibit an influence in interfering with hSOD1 aggregation. It cannot be excluded that there are still similarities in parts of the sequences between the two randomized control peptides and S1VL-21 (e.g., amino acid combinations/positions or charge distributions) that may explain the existing influence on hSOD1 aggregate formation. However, compared to S1VL-21, the randomized control peptides showed a lower affinity to native hSOD1 and significantly less inhibition of aggregate formation.

In summary, we used phage display including control selections and NGS analysis for the identification of peptide ligands for native hSOD1. In this way and together with subsequent characterization methods, we were able to identify S1VL-21 and we showed that this peptide has an impact on hSOD1 aggregation. Further investigations to figure out the binding site of S1VL-21 to hSOD1 are necessary to understand the mechanism of impairment of hSOD1 aggregation. S1VL-21 will be further optimized in order to reduce the required concentration at which the same inhibition rate of aggregate formation is achieved as with S1VL-21 to become a potential lead for drug development.

MATERIALS & METHODS

Protein Expression, Purification, and Reconstitution. Heterologous expression of human SOD1 (hSOD1) in *E. coli* and its purification and fully reconstitution to natively folded dimeric holoenzyme was performed as described previously in Santur et al.[31]

Peptides. Peptide S1VL-21 (YKHSWETQEKQNYVTD-NH_2) as well as its randomized control peptides (S1VL-21_Rdm1: KWYHEEVTYKQDTQNS-NH_2; S1VL-21_Rdm2: YKYVTTENHDSQEQKW-NH_2; S1VL-21_Rdm3: HKSNDKEWTETQQYVY-NH_2) were purchased from Caslo (Lyngby, Denmark) with >98% purity. They are C-terminal-amidated and consist of 16 L-enantiomeric amino acid residues with a molecular mass of 2055 Da.

Phage Display. Phage display with four selection rounds was performed to obtain peptides that specifically bind to native hSOD1. Therefore, 25 μg/mL of dimeric hSOD1 diluted in 100 μL of 50 mM sodium acetate pH 6 was immobilized on a NHS-preactivated surface (3D-NHS 96-well plate, 100 μL functionalization volume, polystyrene; PolyAn, Berlin, Germany) for 1 h at RT. In all selection rounds, the surface was quenched after the hSOD1 solution was removed with 200 μL of quenching solution (50 mM ethanolamine and 100 mM Tris in 10 mM sodium phosphate pH 9) for 1 h at RT followed by five washing steps with 200 μL of washing buffer (150 mM sodium chloride and 0.05% Tween-20 in 50 mM sodium acetate pH 6). In addition before washing, the surface was blocked with 200 μL of 10 mg/mL of bovine serum albumin (BSA) in 50 mM sodium acetate pH 6 in the second round and with 200 μL of 10 mg/mL of milk powder in 50 mM sodium acetate pH 6 in the third round for 15 min at RT to reduce unspecific binding events. During those rounds, 2

https://doi.org/10.1021/acschemneuro.1c00253
ACS Chem. Neurosci. XXXX, XXX, XXX−XXX

mg/mL of BSA or milk powder was added to the washing buffer, respectively. In the first as well as in the fourth round, the surface was not additionally blocked to vary the selection conditions. Then, 2.8 * 10^{11} phages (TriCo-16 phage display peptide library; Creative Biolabs, New York, USA) in 50 mM sodium acetate pH 6 were added and incubated for 30 min at RT in each round. After the nonbinding phages were removed, the well was washed with 200 μL of the respective washing buffer of the corresponding round. The number of washing steps after phage incubation was increased until round 3 (5/10/15/15). Elution of phages was done by incubation with 100 μL of 0.2 M glycine−HCl pH 2.2 for 10 min at RT. The phage-containing solution was then removed from the plate and neutralized by transferring it to a tube containing 25 μL of 1 M Tris-HCl pH 9.1. To determine the output titer, 5 μL of eluted phages were used. Therefore, a dilution series from 10^{-2} to 10^{-8} was prepared with the eluted phages in a total volume of 100 μL in lysogeny broth (LB) medium. Each dilution was mixed with 100 μL of *E. coli* K12 ER2738 (OD_{600} of 0.6) and plated together with 800 μL of top agar on plates (35 × 10 mm; Sarstedt, Nümbrecht, Germany) containing LB-Agar-IPTG-XGal. After overnight incubation at 37 °C, the plaques were counted to determine the output titer.

The remaining eluted phages (120 μL) were amplified in 20 mL of *E. coli* K12 ER2738, starting with an OD_{600} of 0.1, for 4 h at 37 °C. Subsequently, the culture was centrifuged for 20 min at 2700*g* at 4 °C. For phage precipitation, the supernatant was added to 7 mL of PEG-8000/2.5 M sodium chloride, incubated overnight at 4 °C, and centrifuged at 2700*g* at 4 °C for 1 h. The supernatant was discarded, while the phage-containing pellet was dissolved in 1 mL of 1× PBS before another centrifugation at 4 °C and 11 000*g* for 5 min to get rid of residual bacterial components. Afterward, the supernatant was added to 200 μL of PEG-8000/2.5 M sodium chloride and incubated for 1 h on ice followed by a final centrifugation step for 45 min at 2700*g* and 4 °C. The phage-containing pellet was properly resuspended in 100 μL of 1× PBS. The input titer was determined by spectrophotometry[32] in 1× PBS using a 1:10 dilution. The resulting phages were then used in the next selection round with the same phage amount as before and further used for an enrichment ELISA as well as prepared for next-generation sequencing (NGS) analysis.

Besides the main selection with hSOD1 as a target (target selection, TS), two control selections were performed as illustrated in Figure 6

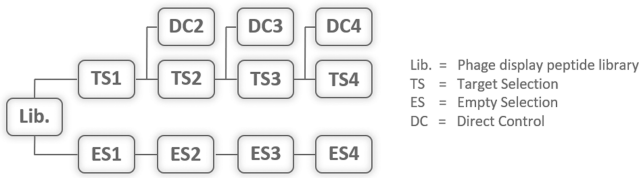

Figure 6. Schematic overview of the phage display selection with target (target selection, TS) and the corresponding control selections empty selection (ES) and direct control (DC) without target. In the first round, the phages from the peptide library are used for the target selection (TS) as well as for the control selection without target called empty selection (ES). One further control without target is performed from the second selection round called direct control (DC), where in contrast to ES, the phages resulting from previous TS are used.

to improve the sequence evaluation efficiency after NGS analysis. The first control selection, called empty selection (ES), was performed in the same way as TS but without hSOD1. During immobilization, 50 mM sodium acetate pH 6 was used instead of hSOD1. All further steps are the same as for TS so that in the end two separate selections with enriched phages were present. One further control was performed starting from the second selection round (direct control, DC). In contrast to ES, here the phages resulting from each round of TS were used for the next selection round that was performed without target protein. After four rounds, four samples for TS and ES (TS1−TS4 and ES1−ES4) and three for DC (DC2−DC4) with enriched phages were present, which were subsequently used together with the phage display peptide library for further analysis.

Enrichment ELISA. An enrichment ELISA was performed to validate the success of the phage display selection. Therefore, 25 μg/mL of dimeric hSOD1 diluted in 100 μL of 50 mM sodium acetate pH 6 was immobilized on an amino plate (Nunc Immobilizer Amino 96-well plate, polystyrene; Thermo Scientific, Waltham, USA) for 1 h at RT. Noncoated wells (50 mM sodium acetate pH 6 without hSOD1) were used as a control for each selection round. The solution was removed, and the surface was quenched with 200 μL of quenching solution (50 mM ethanolamine and 100 mM Tris in 10 mM sodium phosphate pH 9) for 1 h at RT followed by a blocking step with 200 μL of blocking solution (10 mg/mL BSA in 50 mM sodium acetate pH 6) for 15 min at RT. After three washing steps with 200 μL of washing buffer (150 mM sodium chloride, 0.05% Tween-20, 2 mg/mL of BSA in 50 mM sodium acetate pH 6), the amplified and purified phages of each target selection round were diluted in washing buffer to a total amount of 5 * 10^{10} phages in 100 μL. The wells immobilized with hSOD1 as well as noncoated wells were incubated with the corresponding phage solution for 1 h at RT. Unbound phages were removed by three washing steps with 150 μL of washing buffer. The anti-M13 antibody (horseradish peroxidase (HRP)-conjugated mouse monoclonal antibacteriophage M13 antibody; Sino Biological, Peking, China) was diluted 1:2500 in washing buffer, and 100 μL was added into each well for 1 h at RT. After six washing steps with 150 μL of washing buffer, the supernatant was completely removed, 100 μL of the 3,3′,5,5′-tetramethylbenzidine (TMB) solution (TMB was previously dissolved in 1 mL of DMSO and diluted with 9 mL of 0.05 M phosphate citrate buffer pH 5) was added into each well, and after 10 min of incubation at RT, the reaction was stopped with 100 μL of 2 M H_2SO_4. The absorption was quantified at 450 nm using a microplate reader (BMG Labtech, Ortenberg, Germany).

In addition to the samples from the target selection (TS1, TS2, TS3, TS4), the library as well as the wild-type phage without peptide were analyzed. The measurement was performed in double determination. Noncoated wells that were incubated with washing buffer without phages were used as a control for background signal.

Extraction and Amplification of ssM13 DNA for Sequencing. The single-stranded phage DNA from each sample from the phage display selection (all samples from TS, ES, and DC containing enriched phages in 1× PBS as well as the library) were purified and prepared for next-generation sequencing (NGS). Therefore, 10 μL of each input sample was diluted in 600 μL of 1× PBS and incubated with 200 μL of PEG-8000/2.5 M sodium chloride for 20 min at RT after the samples were inverted eight times. The samples were then centrifuged at 20 800*g* for 10 min at 4 °C. The supernatant was removed, and the pellet was carefully resuspended in 200 μL of a 10:1 mixture of 3 M sodium acetate (pH 5.2) and TE. The samples were incubated with 500 μL of 99% ethanol for 15 min at RT before centrifugation at 20 800*g* and 4 °C for 10 min. The supernatant was discarded, and the pellet was washed with 250 μL of 70% ethanol. After a final centrifugation step for again 10 min at 20 800*g* and 4 °C, the supernatant was removed, and the pellet was dried at 30 °C for 8 min before being resuspended in 40 μL of 10 mM Tris pH 8. The concentration of the DNA was determined by the absorption at 260 nm.

The ssDNA was amplified using the KAPA HiFi HotStart ReadyMixPCR Kit (Kapa Biosystems, Wilmington, USA) and the polymerase chain reaction (PCR) for the subsequent NGS. For each 25 ng of phage DNA, 5 μM primers (forward: 5′-TCGTCGGCAG-CGTCAGATGTGTATAAGAGACAGCGCAATTCCTTTAGTGG-TACC-3′, reverse: 5′-GTCTCGTGGGCTCGGAGATGTGTAT-AAGAGACAGCCCTCATAGTTAGCGTAACG-3′) and 12.5 μL of KAPA Hifi Hot Start Ready Mix were added and filled up to 25 μL with ddH_2O. The PCR protocol was composed as follows: initial step at 95 °C for 3 min, followed by 25 cycles with denaturation of DNA at 95 °C for 30 s, annealing at 55 °C for 30 s, and extension at 72 °C for 30 s. A final step of the extension at 72 °C was done for 5 min. The concentration of the amplified DNA was measured by the absorption

https://doi.org/10.1021/acschemneuro.1c00253
ACS Chem. Neurosci. XXXX, XXX, XXX−XXX

at 260 nm and the success of the PCR was evaluated using a 1% agarose gel. Further sample processing and NGS analysis was performed by the Biologisch-Medizinisches Forschungszentrum at the Heinrich Heine University in Düsseldorf, Germany.

Sequence Analysis. The resulting sequencing from the NGS analysis was processed and evaluated with the Target Sequencing Analysis Tool (TSAT), an evaluation software that has been developed by our research group. The use of advanced controls during the phage display selection as well as the establishment of NGS analysis including further sequencing processing via TSAT enabled a high throughput for the identification of target-specific binders.

TSAT is a program that is based on a Python script with front-end access for user. The following modules were used during its creation: Tkinter,[33] Bio,[34] base64,[35] re,[36] collections,[37] sqlite3,[38] time,[39] datetime,[40] sys,[41] and threading.[42]

TSAT screens a given document for the fixed regions directly upstream and downstream of the randomized peptide coding region in the phage genome. The peptide coding sequence is excised and checked for its length. If the length of the nucleotides is dividable by 3, it is translated into the corresponding amino acids. Otherwise, the code is discarded and listed in a document of incomplete sequences. The translated sequences are temporarily saved in a dictionary, which documents the amino acid composition and the total count of each single sequence. For further analysis, the resulting data are transferred to and saved in a data bank. The frequencies of each translated sequence are then normalized to the total number of all translated sequences of the corresponding selection and converted into a parts per million (ppm) format to allow easier comparison between different selections. This is done for each sample of the selection rounds containing the target selection (TS), direct control (DC), and the empty selection (ES) as described in 0. Subsequently, the resulting data from each selection round are compared with each other, whereby only those sequences are considered at the end that have accumulated during the selection starting from the library and that are more or equally frequently present in the TS than in the corresponding ES and DC, respectively. Thus, enriched unspecific binders such as plate binders are removed from the evaluation by directly comparing the selection with target with those without target. The filtered sequences are then assigned two parameters called empty score (EmS) and enrichment factor (EnF). EnF is the frequency of a sequence in the last target selection round divided by the frequency of the same sequence in the library, whereas EmS represents the frequency of a sequence in the last target selection round divided by the frequency of the same sequence in the last empty selection round. As a last step, a scoring list is created based on the EmS values, and the sequences are saved in a FASTA format for the subsequent sequence alignment using the open source software Hammock[43] using default parameters expect that sequence input was done sorted by the EmS values.

Labeling of Native hSOD1 with Fluorophore CF633. CF633 succinimidyl ester (Sigma-Aldrich, St. Louis, USA) was used for labeling native hSOD1 according to the manufacturer's instructions with a few modifications. Therefore, 10 μL of a 50 mM dye stock solution in anhydrous DMSO was added to 190 μL of 180 μM hSOD1 (monomeric concentration) in 50 mM sodium acetate pH 6, which corresponds to a dye/protein molar ration of 15:1 and results in a final concentration of 5% DMSO. All further steps were performed as described in the manufacturer's manual. Free dye was removed by dialysis against 50 mM sodium acetate pH 6. The concentration of labeled CF633-hSOD1 was determined by Bradford assay.[44]

Microscale Thermophoresis Measurements for K_D Determination. In order to determine the equilibration dissociation constant (K_D) of hSOD1 to the selected peptide, microscale thermophoresis (MST) measurements were performed using a Monolith NT.115 blue/red instrument (Nanotemper Technologies, Munich, Germany). Fluorescently labeled hSOD1 (CF633-hSOD1; DOL of 0.5) with a final dimeric concentration of 250 nM was added to samples containing increasing concentrations of unlabeled peptide. Therefore, a 1:1 serial dilution of peptide and a 500 nM CF33-hSOD1 stock solution were prepared in 50 mM sodium acetate pH 6 containing 150 mM sodium chloride and 0.05% Tween-20. The 16 samples were then transferred into specialized glass capillaries (Monolith NT.155 premium capillaries MO-K025; Nanotemper Technologies, Munich, Germany). The measurement was performed at 25 °C using the blue/red channel with an MST and LED power of 40% leading to fluorescence levels between 700 and 900 units. For all experiments, standard parameters were used as recommend by the manufacturer (delay time of heating period of 30 s and re-equilibration period of 5 s). The data were evaluated through the thermophoresis effect using the manufacturer supplied NT analysis software (version 1.5.41).

Thioflavin T Assay. Thioflavin T (ThT) assay was performed to analyze the influence of peptide on hSOD1 fibrillation and/or amyloid-like aggregation. Lyophilized peptides were solved in filtered ddH_2O. Buffers and solutions were then sterile filtered (for larger volumes: Minisart-Plus syringe filter, 0.2 μm, Sartorius, Göttingen, Germany; for smaller volumes: Anotop 10 syringe filter, 0.2 μm, Cytiva, Chicago, USA), while the hSOD1 stock solution in 50 mM sodium acetate buffer pH 6 was centrifuged for 10 min at 20 800g and 21 °C to remove larger particles. Before pipetting together, all components were prewarmed for 1 h at 37 °C. Then, 5 μM dimeric hSOD1 was mixed with 5 μM ThT, 10 mM TCEP, 5 mM EDTA, 150 mM sodium chloride, and the corresponding concentration of peptide (protein/peptide molar ratios of 1:1, 1:2, 1:5, and 1:10 related to the monomeric concentration of hSOD1) in 50 mM sodium acetate buffer pH 6. As controls, a sample with hSOD1 and without peptide and a sample without hSOD1 and with peptide were used. All prepared samples were incubated for 15 min at 37 °C without agitation. Then, 120 μL of each sample was transferred into a well of a 96-well half-area flat-bottom microplate (Corning, New York, USA) containing one 3.2 mm stainless steel bead (Biospec Products, Bartlesville, USA), and the plate was sealed with a foil for 96-well microplates (Thermo Fisher Scientific, Waltham, USA). The progression of fluorescence intensity was measured using a microplate reader (BMG Labtech, Ortenberg, Germany) at 37 °C every 15 min at λ_{ex} = 448−10 nm and λ_{em} = 482−10 nm with 30 s of agitation at 400 rpm before every measurement. The measurements were performed in a 3- to 5-fold determination.

Cell Viability Assay. A cell viability assay using the reduction of 3-(4,5-dimethylthiazol-2-yl)-2,5-diphenyltetrazolium bromide (MTT) was performed to investigate the cytotoxicity of hSOD1 species that were previously incubated with and without S1VL-21 under aggregating conditions. Therefore, Neuro2a cells were cultivated in DMEM medium supplemented with 10% fetal bovine serum (FBS) and 1% penicillin and streptomycin. A total of 2500 cells per well in a volume of 100 μL were seeded on flat-bottomed 96-well plates (VWR, Radnor, USA) and incubated in a 95% humidified atmosphere with 5% CO_2 at 37 °C for 6 h. Aggregates of hSOD1 alone and hSOD1 incubated with increasing concentrations of S1VL-21 (1:1; 1:5; 1:10) under aggregating conditions were prepared as described in 0. The samples were collected after 65 h and centrifuged for 1 h at 4 °C and 100 000g. The supernatant was completely removed, whereas the pellet was dissolved in the same volume of cell culture medium (DMEM containing 10% FBS and 1% penicillin and 1% streptomycin) and diluted to 1:1. Neuro2a cells were then treated with 30 μL of each sample and were further incubated for 3 days in a 95% humidified atmosphere with 5% CO_2 at 37 °C. Cell viability was measured using the Cell Proliferation Kit I according to the manufacturer's instructions (Roche, Basel, Switzerland) in a 5-fold determination. The absorbance of the formazan product was determined by measuring the absorption at 570 nm subtracted by the absorbance at 690 nm in a microplate reader (BMG Labtech, Ortenberg, Germany). The results were normalized to the mean value of cells treated with medium only. As a positive control for cytotoxicity, 10% DMSO diluted in medium was used.

https://doi.org/10.1021/acschemneuro.1c00253
ACS Chem. Neurosci. XXXX, XXX, XXX−XXX

AUTHOR INFORMATION

Corresponding Authors

Jeannine Mohrlüder − *Institute of Biological Information Processing: Structural Biochemistry (IBI-7), Forschungszentrum Jülich, 52425 Jülich, Germany;* orcid.org/0000-0002-9922-2986; Phone: +49-2461-613518; Email: j.mohrlueder@fz-juelich.de

Dieter Willbold − *Institute of Biological Information Processing: Structural Biochemistry (IBI-7), Forschungszentrum Jülich, 52425 Jülich, Germany; Institut für Physikalische Biologie, Heinrich-Heine-Universität Düsseldorf, 40225 Düsseldorf, Germany;* orcid.org/0000-0002-0065-7366; Phone: +49-2461-612100; Email: d.willbold@fz-juelich.de

Authors

Karoline Santur − *Institute of Biological Information Processing: Structural Biochemistry (IBI-7), Forschungszentrum Jülich, 52425 Jülich, Germany; Institut für Physikalische Biologie, Heinrich-Heine-Universität Düsseldorf, 40225 Düsseldorf, Germany*

Elke Reinartz − *Institut für Physikalische Biologie, Heinrich-Heine-Universität Düsseldorf, 40225 Düsseldorf, Germany*

Yi Lien − *Institute of Biological Information Processing: Structural Biochemistry (IBI-7), Forschungszentrum Jülich, 52425 Jülich, Germany*

Markus Tusche − *Institute of Biological Information Processing: Structural Biochemistry (IBI-7), Forschungszentrum Jülich, 52425 Jülich, Germany*

Tim Altendorf − *Institute of Biological Information Processing: Structural Biochemistry (IBI-7), Forschungszentrum Jülich, 52425 Jülich, Germany; Institut für Physikalische Biologie, Heinrich-Heine-Universität Düsseldorf, 40225 Düsseldorf, Germany*

Marc Sevenich − *Institute of Biological Information Processing: Structural Biochemistry (IBI-7), Forschungszentrum Jülich, 52425 Jülich, Germany; Institut für Physikalische Biologie, Heinrich-Heine-Universität Düsseldorf, 40225 Düsseldorf, Germany*

Gültekin Tamgüney − *Institute of Biological Information Processing: Structural Biochemistry (IBI-7), Forschungszentrum Jülich, 52425 Jülich, Germany; Institut für Physikalische Biologie, Heinrich-Heine-Universität Düsseldorf, 40225 Düsseldorf, Germany*

Complete contact information is available at: https://pubs.acs.org/10.1021/acschemneuro.1c00253

Author Contributions

K.S. contributed to the design of the TSAT software, contributed to the design of experiments, performed most of the experiments, analyzed data, and wrote the initial draft of the manuscript; E.R. contributed to the design of experiments and provided feedback on experimental results; Y.L. and M.T. performed cell cultivation; T.A. contributed to the design of TSAT and edited the manuscript; M.S. contributed to the design of TSAT; G.T. contributed to the design of the cell viability assay as well as provided feedback on experimental results; J.M. contributed to the study conception and design and edited the manuscript; D.W. designed the overall study and edited the manuscript. All authors contributed to the preparation of this manuscript as well as read and approved the final manuscript.

Notes

The authors declare no competing financial interest.

ACKNOWLEDGMENTS

The authors wish to express their thanks to the Biologisch-Medizinisches Forschungszentrum of the Heinrich Heine University Düsseldorf for performing the NGS analysis.

REFERENCES

(1) Bento-Abreu, A., Van Damme, P., Van Den Bosch, L., and Robberecht, W. (2010) The neurobiology of amyotrophic lateral sclerosis. *Eur. J. Neurosci 31*, 2247−2265.

(2) Sreedharan, J., and Brown, R. H., Jr (2013) Amyotrophic lateral sclerosis: problems and prospects. *Ann. Neurol. 74*, 309−316.

(3) Grad, L. I., Rouleau, G. A., Ravits, J., and Cashman, N. R. (2017) Clinical spectrum of amyotrophic lateral sclerosis (ALS). *Cold Spring Harbor Perspect. Med. 7*, a024117.

(4) Gordon, P. H. (2013) Amyotrophic lateral sclerosis: an update for 2013 clinical features, pathophysiology, management and therapeutic trials. *Aging Dis 04*, 295−310.

(5) Zhao, B., Marciniuk, K., Gibbs, E., Yousefi, M., Napper, S., and Cashman, N. R. (2019) Therapeutic vaccines for amyotrophic lateral sclerosis directed against disease specific epitopes of superoxide dismutase 1. *Vaccine 37*, 4920−4927.

(6) Baskoylu, S. N., Yersak, J., O'Hern, P., Grosser, S., Simon, J., Kim, S., Schuch, K., Dimitriadi, M., Yanagi, K. S., Lins, J., et al. (2018) Single copy/knock-in models of ALS SOD1 in C. elegans suggest loss and gain of function have different contributions to cholinergic and glutamatergic neurodegeneration. *PLoS Genet. 14*, No. e1007682.

(7) Rosen, D. R., Siddique, T., Patterson, D., Figlewicz, D. A., Sapp, P., Hentati, A., Donaldson, D., Goto, J., O'Regan, J. P., Deng, H. X., et al. (1993) Mutations in Cu/Zn superoxide-dismutase gene are associated with familial amyotrophic-lateral-sclerosis. *Nature 362*, 59−62.

(8) Valentine, J. S., Doucette, P. A., and Zittin Potter, S. (2005) Copper-zinc superoxide dismutase and amyotrophic lateral sclerosis. *Annu. Rev. Biochem. 74*, 563−593.

(9) Roe, J. A., Butler, A., Scholler, D. M., Valentine, J. S., Marky, L., and Breslauer, K. J. (1988) Differential scanning calorimetry of Cu,Zn-superoxide dismutase, the apoprotein, and its zinc-substituted derivatives. *Biochemistry 27*, 950−958.

(10) Rodriguez, J. A., Valentine, J. S., Eggers, D. K., Roe, J. A., Tiwari, A., Brown, R. H., Jr, and Hayward, L. J. (2002) Familial amyotrophic lateral sclerosis-associated mutations decrease the thermal stability of distinctly metallated species of human copper/zinc superoxide dismutase. *J. Biol. Chem. 277*, 15932−15937.

(11) Reaume, A. G., Elliott, J. L., Hoffman, E. K., Kowall, N. W., Ferrante, R. J., Siwek, D. F., Wilcox, H. M., Flood, D. G., Beal, M. F., Brown, R. H., Jr, et al. (1996) Motor neurons in Cu/Zn superoxide dismutase-deficient mice develop normally but exhibit enhanced cell death after axonal injury. *Nat. Genet. 13*, 43−47.

(12) Jonsson, P. A., Graffmo, K. S., Brannstrom, T., Nilsson, P., Andersen, P. M., and Marklund, S. L. (2006) Motor neuron disease in mice expressing the wild type-like D90A mutant superoxide dismutase-1. *J. Neuropathol. Exp. Neurol. 65*, 1126−1136.

(13) Graffmo, K. S., Forsberg, K., Bergh, J., Birve, A., Zetterstrom, P., Andersen, P. M., Marklund, S. L., and Brannstrom, T. (2013) Expression of wild-type human superoxide dismutase-1 in mice causes amyotrophic lateral sclerosis. *Hum. Mol. Genet. 22*, 51−60.

(14) van Zundert, B., and Brown, R. H., Jr (2017) Silencing strategies for therapy of SOD1-mediated ALS. *Neurosci. Lett. 636*, 32−39.

(15) Bosco, D. A., Morfini, G., Karabacak, N. M., Song, Y., Gros-Louis, F., Pasinelli, P., Goolsby, H., Fontaine, B. A., Lemay, N., McKenna-Yasek, D., et al. (2010) Wild-type and mutant SOD1 share an aberrant conformation and a common pathogenic pathway in ALS. *Nat. Neurosci. 13*, 1396−1403.

(16) Forsberg, K., Jonsson, P. A., Andersen, P. M., Bergemalm, D., Graffmo, K. S., Hultdin, M., Jacobsson, J., Rosquist, R., Marklund, S. L., and Brannstrom, T. (2010) Novel antibodies reveal inclusions containing non-native SOD1 in sporadic ALS patients. *PLoS One 5*, No. e11552.
(17) Forsberg, K., Andersen, P. M., Marklund, S. L., and Brannstrom, T. (2011) Glial nuclear aggregates of superoxide dismutase-1 are regularly present in patients with amyotrophic lateral sclerosis. *Acta Neuropathol. 121*, 623−634.
(18) Grad, L. I., Yerbury, J. J., Turner, B. J., Guest, W. C., Pokrishevsky, E., O'Neill, M. A., Yanai, A., Silverman, J. M., Zeineddine, R., Corcoran, L., et al. (2014) Intercellular propagated misfolding of wild-type Cu/Zn superoxide dismutase occurs via exosome-dependent and -independent mechanisms. *Proc. Natl. Acad. Sci. U. S. A. 111*, 3620−3625.
(19) Chia, R., Tattum, M. H., Jones, S., Collinge, J., Fisher, E. M., and Jackson, G. S. (2010) Superoxide dismutase 1 and tgSOD1 mouse spinal cord seed fibrils, suggesting a propagative cell death mechanism in amyotrophic lateral sclerosis. *PLoS One 5*, No. e10627.
(20) Furukawa, Y., Kaneko, K., Watanabe, S., Yamanaka, K., and Nukina, N. (2013) Intracellular seeded aggregation of mutant Cu,Zn-superoxide dismutase associated with amyotrophic lateral sclerosis. *FEBS Lett. 587*, 2500−2505.
(21) Grad, L. I., Pokrishevsky, E., Silverman, J. M., and Cashman, N. R. (2014) Exosome-dependent and independent mechanisms are involved in prion-like transmission of propagated Cu/Zn superoxide dismutase misfolding. *Prion 8*, 331−335.
(22) Rakhit, R., Crow, J. P., Lepock, J. R., Kondejewski, L. H., Cashman, N. R., and Chakrabartty, A. (2004) Monomeric Cu,Zn-superoxide dismutase is a common misfolding intermediate in the oxidation models of sporadic and familial amyotrophic lateral sclerosis. *J. Biol. Chem. 279*, 15499−15504.
(23) Ding, F., Furukawa, Y., Nukina, N., and Dokholyan, N. V. (2012) Local unfolding of Cu, Zn superoxide dismutase monomer determines the morphology of fibrillar aggregates. *J. Mol. Biol. 421*, 548−560.
(24) Lai, Z., Colon, W., and Kelly, J. W. (1996) The acid-mediated denaturation pathway of transthyretin yields a conformational intermediate that can self-assemble into amyloid. *Biochemistry 35*, 6470−6482.
(25) Wiseman, R. L., Johnson, S. M., Kelker, M. S., Foss, T., Wilson, I. A., and Kelly, J. W. (2005) Kinetic stabilization of an oligomeric protein by a single ligand binding event. *J. Am. Chem. Soc. 127*, 5540−5551.
(26) van Groen, T., Schemmert, S., Brener, O., Gremer, L., Ziehm, T., Tusche, M., Nagel-Steger, L., Kadish, I., Schartmann, E., Elfgen, A., et al. (2017) The Abeta oligomer eliminating D-enantiomeric peptide RD2 improves cognition without changing plaque pathology. *Sci. Rep. 7*, 16275.
(27) Kutzsche, J., Schemmert, S., Tusche, M., Neddens, J., Rabl, R., Jurgens, D., Brener, O., Willuweit, A., Hutter-Paier, B., and Willbold, D. (2017) Large-scale oral treatment study with the four most promising D3-derivatives for the treatment of Alzheimer's disease. *Molecules 22*, 1693.
(28) Schemmert, S., Schartmann, E., Zafiu, C., Kass, B., Hartwig, S., Lehr, S., Bannach, O., Langen, K. J., Shah, N. J., Kutzsche, J., et al. (2019) Abeta oligomer elimination restores cognition in transgenic Alzheimer's mice with full-blown pathology. *Mol. Neurobiol. 56*, 2211−2223.
(29) Abdolvahabi, A., Shi, Y. H., Rasouli, S., Croom, C. M., Chuprin, A., and Shaw, B. F. (2017) How do gyrating beads accelerate amyloid fibrillization? *Biophys. J. 112*, 250−264.
(30) Naiki, H., Higuchi, K., Hosokawa, M., and Takeda, T. (1989) Fluorometric-determination of amyloid fibrils invitro using the fluorescent dye, thioflavine-T. *Anal. Biochem. 177*, 244−249.
(31) Santur, K. B., Sevenich, M. M., Schwarten, M., Nischwitz, V., Willbold, D., and Mohrluder, J. (2018) In vitro reconstitution of the highly active and natively folded recombinant human superoxide dismutase 1 holoenzyme. *Chemistryselect 3*, 7627−7632.
(32) Casadevall, A., and Day, L. A. (1982) DNA packing in the filamentous viruses fd, Xf, Pf1 and Pf3. *Nucleic Acids Res. 10*, 2467−2481.
(33) Lundh, F. (1999) An introduction to Tkinter, https://docs.python.org/3/library/tkinter.html.
(34) Cock, P. J. A., Antao, T., Chang, J. T., Chapman, B. A., Cox, C. J., Dalke, A., Friedberg, I., Hamelryck, T., Kauff, F., Wilczynski, B., et al. (2009) Biopython: freely available Python tools for computational molecular biology and bioinformatics. *Bioinformatics 25*, 1422−1423.
(35) base64 — Base16, Base32, Base64, Base85 Data Encodings, https://docs.python.org/3/library/base64.html?highlight=base64#module-base64.
(36) re — regular expression operations, https://docs.python.org/3/library/re.html?highlight=re#module-re.
(37) collections — container datatypes, https://docs.python.org/3/library/collections.html?highlight=collections#module-collections.
(38) Hipp, D. R. (2020) SQLite, https://www.sqlite.org/index.html.
(39) time — time access and conversions, https://docs.python.org/3/library/time.html.
(40) datetime — basic date and time types, https://docs.python.org/3/library/datetime.html?highlight=datetime#module-datetime.
(41) sys — system-specific parameters and functions, https://docs.python.org/3/library/sys.html?highlight=sys#module-sys.
(42) threading — thread-based parallelism, https://docs.python.org/3/library/threading.html.
(43) Krejci, A., Hupp, T. R., Lexa, M., Vojtesek, B., and Muller, P. (2016) Hammock: a hidden Markov model-based peptide clustering algorithm to identify protein-interaction consensus motifs in large datasets. *Bioinformatics 32*, 9−16.
(44) Bradford, M. M. (1976) A rapid and sensitive method for the quantitation of microgram quantities of protein utilizing the principle of protein-dye binding. *Anal. Biochem. 72*, 248−254.

https://doi.org/10.1021/acschemneuro.1c00253
ACS Chem. Neurosci. XXXX, XXX, XXX−XXX